Atlantis Highlights in Computer Sciences, volume 4
Proceedings of the 3rd International Conference on Integrated Intelligent Computing Communication & Security (ICIIC 2021)

A Hybrid Hierarchical Sparse Kernel Classification Model for Remote Sensing Image Retrieval

Sudha S K[1,*], Aji S[2]

[1,2]*Research Centre, Department of Computer Science, University of Kerala, Kariavattom, Thiruvananthapuram - 695581, Kerala, India*
[*]*Corresponding author. Email: sudha.krishnaa@keralauniversity.ac.in*

ABSTRACT
In remote sensing applications, finding matching images across huge datasets is difficult due to the scarcity of annotated images. The high spatio-spectral resolution and high-dimensional sparse nature make the remote sensing images difficult to utilize in particular applications. Hence, competent retrieval methods are to be designed with efficient classification strategies that solve multiclass problems. This work incorporates developing a new hybrid hierarchical sparse kernel classification (HHSKC) method using relevance vector machine (RVM) and support vector machine (SVM) classifiers. The feature extraction is attained through a relational autoencoder (RAE) with proper dimensionality reduction. The excellent competing qualities of the hybrid classifiers and the deep feature representations improve the overall potential of the RAE-HHSKC framework. The proposed RAE-HHSKC is validated on two benchmark RS image datasets: the UC Merced (UCMD) dataset and the RS-19 dataset. The RAE-HHSKC framework obtained state-of-the-art results using both sparse kernel learning machines (SKLM) and deep features.

Keywords: *Hybrid Classification, Relational Autoencoder, Relevance Vector Machine, Remote Sensing Image Retrieval, Support Vector Machine.*

1. INTRODUCTION

Retrieval of visually identical images from large-scale remote sensing (RS) databases is an essential application of content-based image retrieval (CBIR) applications. The remote sensing image retrieval (RSIR) uses visual contents from the input images to retrieve similar image set from very large databases. RSIR models need more sufficiently labeled training samples to perform correctly, which is challenging [1]. Remote sensing images (RSI) are being used in a broad spectrum of applications like change detection, glacier monitoring, land-cover classification, object detection, and retrieval. Due to satellite technology advancement, remote sensors are providing huge volumes of data with very high spectral, spatial, temporal, and radiometric resolution. Such an increase requires significant modifications in the approach we use and manage the RSI. Also, RS images are large and are taken from high altitudes compared with ordinary images. As a result, there are many heterogeneous objects in one image, making the structure highly complex. These challenges add multiple complications to the RSI analysis, especially in RSIR tasks. Hence, more competing and efficient RSIR models are to be formulated to deal with the high dimensionality and spatio-spectral complexity for recognizing a similar class.

During the last decades, several RSIR frameworks have been recommended [2-4]. However, the launch of deep learning (DL) approaches in RS scenario presents new challenges to tackle. Many DL-based retrieval frameworks are available [5-10], using different architectures and learning strategies. Generally, an RSIR framework incorporates a feature extraction and a retrieval phase that includes an efficient classification module for labeling. The feature extraction phase in a retrieval model is turned to be extensively important as data expands high dimensional.

The classifier framework is designed in such a way as to minimize the labeling cost. The capabilities of both the feature extraction and the classification phase make the RSIR framework efficient in performance. The use of a hybrid approach classification has been found to be suitable for the high-dimensional RS data and generate classification that is often more accurate than the individual classification schemes.

The core idea of this proposed work is to design an efficient RSIR framework, which uses a relational autoencoder in the feature extraction phase, which preserves the data relationships. The classification environment is designed in a hybrid fashion using the relevant vector machine and support vector machine. Hence, the classifier performs much faster at the testing phase when using RVM than using SVM. The main attraction of using SVM is that its target function attempts in minimizing the errors on training data. Also, simultaneously it maximizes the margin between the two classes in the higher dimensional feature space implicitly defined by the kernel. This is highly effective for avoiding overfitting, which leads to good generalization. Furthermore, the classification results in a sparse model, dependent only on a subset of kernel functions. Also, the SVM is generally optimized to achieve excessive-class reliability for classifying highly overlapping classes.

Hence, a hybrid hierarchical sparse kernel classification (HHSKC) framework is formulated here using the two SKLM- the relevance vector machine and the support vector machine using the RAE features. The framework incorporates the sparse kernel properties of both RVM and SVM for an efficient RSI classification. The major contributing factors of this work are:

i. the design of an RSIR consisting of a deep feature learning (DFL) phase. The DFL generates features with dimensionality reduction using an RAE, which preserves the relationships between the data points.

ii. the design of an HHSKC framework with improved classification accuracy to provide better retrieval results.

The sections of this work are arranged as below. A detailed background of the related works is presented in Section 2. A description of the RAE-HHSKC framework is detailed in Section 3. The results obtained using the RAE-HHSKC framework based on two well-known RS datasets are narrated in Section 4. A concluding remark is presented in Section 5.

2. BACKGROUND AND RELATED WORKS

The performance of remote sensing image retrieval models mainly depends on the expressive power of image features. The RSIR methods already available use low-level features or hand-crafted features, like color [11-13], texture [11-13], and shape [11]. Some representative features based models, like the scale invariant feature transform (SIFT) [14-16], color correlogram [12,13], local binary pattern (LBP) [16,18], grey level co-occurrence matrix (GLCM) [12,13,17], histogram of oriented gradients (HOG) [18], Gabor filters [18], or their variants are also found used. Some mid-level feature representations, like the well-known bag-of-visual-words (BoVW) model, are also been extensively popular in the RS communities [19,20] for their simplicity.

The recent works on RSIR using deep feature representations for interpreting the patterns [21-23] are more powerful. A novel result ranking loss (RRL) method is proposed in [24], an RSIR using fuzzy rules, and a fuzzy distance is developed in [25]. A classification-similarity network and double fusion model is designed in [26]. An RSIR framework for zero-shot intermodal data was proposed in [27]. A global-aware ranking loss (GRL) model is proposed in [28].

Most of the recent frameworks use convolution neural networks (CNN) and autoencoders (AE) as the DL architecture. More recently, autoencoders have attracted center stage in the *deep architecture* approaches [29]. Hence, the AE and its variants are recently used for deep features extraction [30]. Being a neural network-based feature extraction method, AE achieves great accomplishment in generating robust features of high-dimensional data. However, they fail to consider the relationships maintained between data samples, which severely affects the overall effectiveness of the retrieval models. Hence, this work incorporates designing a relational autoencoder (RAE) [31] for extracting the most representative deep features, which considers both data features and respective relations.

For the RSIR, excellent efforts are made to establish robust and stable image classification methods. Hybrid classification systems are very promising for producing better outcomes by integrating the successful features of various classifiers. Many hybrid classification strategies are proposed in RSI literature [32, 33]. Support vector machines (SVM) [34] and relevance vector machines (RVM) [35] constitute two state-of-the-art sparse kernel learning (SKLM) machines. The RVM is a Bayesian extension of the support vector machine (SVM) that has considerable potential for analyzing remotely sensed data [36]. In these years, it is reported that RVM is as powerful as SVM [37] for image classification applications. Key attractions of the RVM are (i) it is less responsive to the hyperparameter settings, (ii) not restricted by the Mercer kernels, and (iii) the provision for a probabilistic output and considerably fewer relevance vectors for a specific analysis [38]. The RVM achieves sparsity because of its posterior distributions of the weights that are sharply peaked around zero. Those training vectors associated with the remaining nonzero weights are called the relevance vectors (RV).

Based on the review and analysis, it is understood that several RSIR frameworks exist that are most promising and prevailing, but further researches have to be initiated to develop new highly performance-oriented RSIR frameworks that can compete with the state-of-the-art methods.

3. THE RAE-HHSKC MODEL PIPELINE

This work aimed at the design of an RSIR framework called RAE-HHSKC using deep features**.** The framework includes two phases- i) a DFL using relational autoencoder and ii) a classification phase using a hybrid hierarchical sparse kernel learning RVM and SVM for obtaining a relatively sparse solution. The deep feature set is extracted using the RAE, preserving the affinity among the data points with reduced dimensionality. The extracted deep features are used for classification using the hybrid framework. Figure 1. illustrates the phases involved in the recommended RAE-HHSKC model.

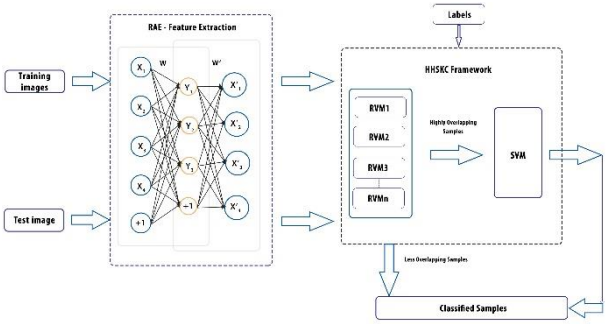

Figure 1 Illustration of the RAE-HHSKC Framework

The HHSKC works in two levels of hierarchy. The first level utilizes the probabilistic nature of several binary RVM models. The RVM determines the samples to be retained and those identified for the second phase of classification. The RVM interprets the probabilistic output classification as a *confidence* measure, as a symmetrical interval concerning the origin ([−range, range]), where RVM discovers lower *confidence*, which is influenced by the conditional probability as in (11). These choices of training samples fall below the logistic curve to be identified as hard-to-classify samples and given for the second level of SVM classification [46].

A testing sample is first classified by the RVM that exhibited more *confidence* by assigned its posterior probabilities in the training phase. The testing ends when the samples are classified outside the interval [−range, range]; otherwise, the SVM will perform the classification. As the range value increases, fewer and non-overlapping samples are classified using the RVM. The more and hard-to-classify highly overlapping samples are classified by the SVM in the next level [47].

3.1 Deep Feature Learning using RAE

The objective of a basic autoencoder (BAE) is to learn and regenerate the input data with reduced dimensionality. An autoencoder comprises three layers: i) input layer, ii) encoder layer, and iii) decoder layer. In the encoding phase, the input is usually mapped in the lower dimensional features space with a constructive representation. This approach can be repeated until the desired feature dimensional space is reached. Whereas in the decoding phase, the actual features are regenerated from lower dimensional features with reverse processing. But the basic AE fails to preserve the data relationship, which is essential in expressing the input. Hence, a choice of RAE is incorporated for the DFL in an unsupervised manner. A weight function is added to preserve the data relationship. Maintaining the mutual relationships between data samples makes AE sensitive even to slight changes. Hence, preserving the relationships achieves an improved performance of AE with reduced dimensionality [48-51]. Therefore, an RAE is aiming at the reduction of the loss in the regeneration of data and their relationships. For an input data *X* with *n* samples and *m* features, the encoder output *Y* is the reduced version of *X*. Then, the decoder regenerates the input *X* from the encoder representation *Y* by reducing the difference between *X* and X'.

$$Y = f(X) = s_f(WX + bX) \quad (1)$$

where s_f is an activation function, which is nonlinear. A weight matrix W and a bias vector $b \in R^n$ are the encoder parameters. Then the decoder-function g is expressed as Eqn. (2).

$$X' = g(Y) = s_g(W'Y + b_Y) \quad (2)$$

where s_g is the activation function for the decoder, and b_Y is the bias vector.

During training, the autoencoder finds parameters $\theta = W, b_X + b_Y$ that reduce the regeneration loss on the given dataset *X* with an objective function as in Eqn. (3).

$$Obj_{BAE} = \min_{\theta} L(X, X') = \min_{\theta} L(X, g(f(X))) \quad (3)$$

For linear regeneration, the loss (L1) is the squared-error (Eqn. (4)), and for nonlinear regeneration, the loss (L2) is from the cross-entropy (Eqn. (5)).

$$L1(\theta) = \sum_{i=1}^{n} \|x_i - x'_i\|^2 = \sum_{i=1}^{n} \|x_i - g(f(x_i))\|^2 \quad (4)$$

$$L2(\theta) = -\sum_{i=1}^{n} [x_i \log(y_i) + (1 - x_i)\log(1 - y_i)] \quad (5)$$

where $x_i \in X, x'_i \in X' and\ y_i \in Y$. Hence, the Obj_{RAE} can be written as Eqn. (6).

$$Obj_{RAE} = (1 - \alpha) \min_{\theta} L(X, X') + \alpha \min_{\theta} L(R(X), R(X')) \quad (6)$$

where $R(X)$ is the relationship between data samples in *X*, and $R(X')$ is the relationship between data samples in *X'*. The parameter α maintains the weight value of loss in the data and the relationship, and θ is a neural network parameter of the AE. The data relations are managed by their similarities, where *R(X)* is the multiplied value of *X* and X^T . Then, the objective function can take the following form as Eqn. (7).

$$Obj_{RAE} = (1-\alpha)\min_{\theta} L(X, X') + \alpha \min_{\theta} L(XX^T, X'X'^T) \quad (7)$$

A rectified linear unit (ReLU) activation function is used for an improvement in the computational efficiency and filter out unnecessary relations, which controls the weights-of-similarities.

$$\tau_t(r_{ij}) = \begin{cases} r_{ij}, & if\ r_{ij} \geq t, \\ 0, & otherwise, \end{cases} \quad (8)$$

where *t* is a threshold value used to filter out weak and irrelevant relationships. Then the objective function of RAE is defined as Eqn. (9).

$$Obj_{RAE} = (1-\alpha)\min_{\theta} L(X, X') + \alpha \min_{\theta} L(\tau_t(XX^T, \tau_t X'X'^T)) \quad (9)$$

The RAE iteratively learns from input data using ReLU. The ReLU typically learns the features much faster from the original data in an unsupervised manner. The RAE defines a loss function L and initializes the neural network by iteratively adding layers subject to the input data and the activation function. The RAE is trained by using stochastic gradient descent (SGD) until convergence [52]. It is noticed that preserving data relationships contributes to the decrease of regeneration loss. Thus, the RAE generates robust and meaningful deep features with minimal information loss and reduced dimensionality and is further used in the classification framework [53].

3.2 Hybrid Hierarchical Sparse Kernel Classification

Hybrid architecture is always leveraged in obtaining precise classification accuracies. The hybrid hierarchical sparse kernel classification (HHSKC) framework using an RVM and SVM is recommended to obtain an efficient RSIR. The sparse kernel properties of both the RVM and SVM make the model efficient for the RSI classification avoiding overfitting. An RVM is engaged in determining the less confident classified samples in the HHSKC framework, and the next hierarchy uses an SVM to classify the highly overlapping classes.

3.2.1 Relevance Vector Machine

The RVM acquires a sparse solution with a generalization ability equivalent to the SVM, which benefited from the kernel and sparse properties. For designing a multiclass retrieval model, the RVM is used either in a one-against-one (OAO) or one-against-all (OAA) fashion. The multiclass RVM consists of multiple independent binary classifiers. The RVM learning technique uses a chunk of sample input vectors and the respective target class labels [54-58]. The RVM tries to catch a hyperplane as a 'weighted' combination. The RVM makes predictions conditioned on the function given in Eqn. (10).

$$f(x) = \sum_{i=1}^{N} \omega_i\, k\langle x, x_i\rangle + w_0 \quad (10)$$

where w_0 shows the model weight, and $k\langle x, x_i\rangle$ is a kernel function effectively. The parameters ω_i (for $i = 1$ to N) in $f(x)$ are decided by the Bayesian estimation, introducing a sparse prior on ω_i. RVM classifier models the probability distribution of its class label, and the classification is carried out by predicting the posterior probability given as Eqn. (11).

$$P\left(\frac{y}{f(x)}\right) = \frac{1}{1+e^{-f(x)}} \quad (11)$$

where, $P\left(\frac{y}{f(x)}\right)$ is the conditional probability. The parameter ω_i is attained by maximizing the posterior distribution of class labels given the input vectors. The RVM works as a fully probabilistic framework to avoid overfitting. It also introduces a prior over the model weights governed by a set of hyperparameters, one associated with each weight, w. The parameter w is then distributed as in Eqn. (12).

$$P(w/\omega) = \prod_{i=1}^{N} N(w_i/0, \omega_i^{-1}) \quad (12)$$

During the optimization process, many hyperparameters will have large values, and, thus, most posterior probabilities of the corresponding model weights will be zero, which realizes sparsity. The training samples with small nonzero coefficients ω_i are the relevance vectors (RV) and are promoted for classification contributing to the decision function $f(x)$.

3.2.2 Support Vector Machine

The SVM is aimed to find a hyperplane that optimally separates the positive and negative samples. The optimal hyperplane gives the maximum margin between the training samples that are nearest to it. The support vectors (SV) lie closest to the separating hyperplane [59]. Once this hyperplane is found, new samples can be classified simply by determining on which side of the hyperplane they fall, and the decision boundary is chosen to be the one for which the margin is maximized. Maximizing the margin is viewed as an optimization problem:

$$\min_{\hat{w}^i, b, \varepsilon} J(\hat{w}^i, b, \varepsilon) = \frac{1}{2}(\hat{w}^i)^T \hat{w}^i + \gamma \sum_{i=1}^{N} \varepsilon_j^i \quad (13)$$

subject to:

$$(\hat{w}^i)^T \varphi(x_j) + b^i \geq 1 - \varepsilon_j^i, y_j = i, \quad (14)$$

$$(\hat{w}^i)^T \varphi(x_j) + b^i \leq -1 + \varepsilon_j^i, y_j \neq i \quad (15)$$

where, w is a normal vector of the hyperplane, b is a bias, $\varphi(x_j)$ is a nonlinear function that maps x to a high-dimensional feature space, ε is the error in

misclassification, and γ is a regularization constant that controls the tradeoff between the classification margin and cost of misclassification. Once the SVM models have been solved, the class label of a testing example x can be predicted as in Eqn. (16).

$$y(x) = arg_{i=1,2,\ldots C}\max(((\hat{w}^i)^T\varphi(x) + b^i \qquad (16)$$

4. EXPERIMENTS AND RESULTS

Two benchmark RS datasets, namely the UCMD [38] and RS-19 [39], are used for evaluating the overall performance of the RAE-HHSKC framework. The UCMD contains 21 Land-Use/Land-Cover (LULC) categories of high-resolution aerial images. Each class contains 100 image samples with a pixel resolution of 0.3 m. and size 256 × 256. The RS-19 dataset contains 19 classes of satellite scenes from Google Earth. Each class has about 50 RGB image samples with a size of 600 × 600. Both the datasets are challenging with many overlapping classes. The test data is randomly split into train and test set with 80% and 20%, respectively.

The RAE extracts the robust deep features with reduced dimensionality, which are then recognized by the HHSKC framework for classification. The training of RAE involves finding three groups of parameters W, b_X and b_Y, that reduce the regeneration loss using stochastic gradient descent (SGD) for 100 epochs. The necessary number of neurons in each layer is decided as in [31].

The parameter α controls the weights of the loss in the regeneration process. The classification is accomplished in two levels which use the probabilistic nature of RVM to determine hard-to-classify samples. A *confidence* interval range [-10,10] is chosen for the RVM classification phase. The hard-to-classify, highly overlapping samples are then trained by a performance-oriented SVM to attain high classification efficiency. The radial basis function (RBF) kernel is employed in both RVM and SVM in the experiment.

4.1 Evaluating the Deep Feature Learning

The stability of extracted features is assessed by measuring the regeneration loss using mean squared error (MSE) for different α values. The MSE obtained for the UCMD and RS-19 datasets using different α values is plotted in Figure 2.

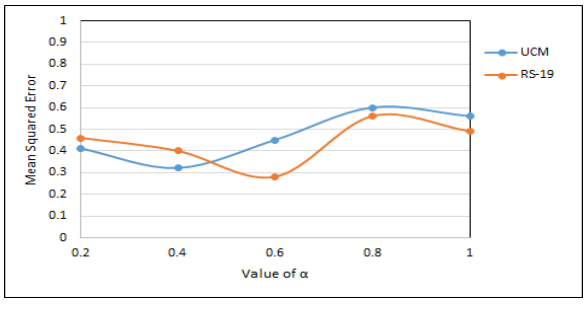

Figure 2 MSE Vs. α

An increased α value results in increased information loss because the model tries to concentrate more on maintaining relationship regeneration. Hence an acceptable value is chosen to maintain the data and relationship regeneration. The α value noted in our experiment for the UCMD is 0.4 and 0.6 for the RS-19 datasets, respectively, for better performance.

4.2 Evaluating Retrieval Performance

The overall retrieval efficiency of the RAE-HHSKC framework is measured by the standard evaluation metrics like precision (P), recall (R), F1-score, and average normalized modified retrieval rank (ANMRR). The query images for retrieval are randomly selected from the test dataset. The per-class P-R values obtained for the UCMD and the RS-19 datasets are represented in Figures 3 and 4, respectively.

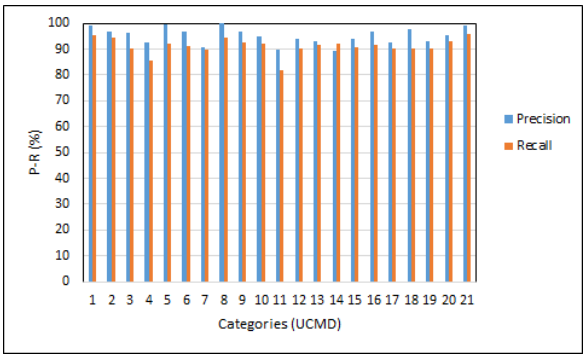

Figure 3 Per-Class P-R values for UCMD

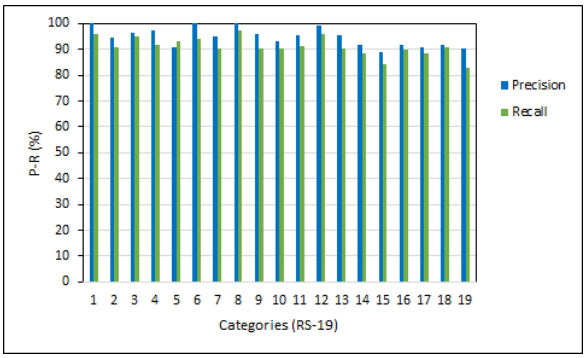

Figure 4 Per-Class P-R values for RS-19

For both datasets, the RAE-HHSKC framework achieved a better response in precision, assuring that relevant images are retrieved from the entire dataset. The slight fall in the recall is by means of the highly overlapping behavior of the datasets. The average precision, recall, F1-score, and ANMRR values obtained for UCMD and RS-19 are plotted in Table 1. respectively.

Table 1. Precision, Recall F1-Score and ANMRR

Dataset	Precision	Recall	F1-Score	ANMRR
UCMD	95.15	91.24	93.13	0.269
RS-19	94.59	91.04	92.77	0.298

4.3 Comparison with Current Methods

The overall efficiency of the RAE-HHSKC framework in terms of ANMRR values obtained for the UCMD dataset against other available methods [40-44] are plotted in Table 2. The results indicate that using the RAE-HHSKC framework achieved competing performance with some state-of-the-art DL-based frameworks.

Table 2. Comparison of ANMRR values for UCMD

Method	ANMRR
LBP+KNN [40]	0.8523
SIFT+KNN [40]	0.7645
SIFT+3 Layer Graph [41]	0.5366
VGGM-FC2 [44]	0.378
SGCN [42]	0.3
SBS-CNN [6]	0.2683
ReCNN+ [43]	0.264
Proposed Method	**0.269**

The RAE-HHSKC framework attains better ANMRR values by using the robust feature set extracted, preserving the data relationships. The ANMRR values obtained for the RS-19 dataset against other available methods are plotted in Table 3.

Table 3. Comparison of ANMRR values for RS-19

Method	ANMRR
CaffeNet +FC6 [45]	0.190
VGG-M+FC6 [45]	0.197
VGG-VD19+ FC6 [45]	0.232
GoogLeNet [45]	0.243
Proposed Method	**0.298**

The overall results show that the proposed RAE-HHSKC framework generates competing results with the DL-based approaches.

It is realized that the robust and meaningful features generated using RAE with minimal information loss are vital factors in achieving good classification results. The HHSKC framework works in two levels by which the hard-to-classify, highly overlapping classes are identified using the relevant vectors and support vectors. Usually, the number of SV identified during training highly influences the performance of the SVM classifier phase. The RVM classification phase in the HHSKC framework identifies the less overlapping samples, and hence, a reduction in the number of SV is recognized, which improves the overall performance.

As a summary, this work contributes to designing a hybrid hierarchical sparse kernel classification framework using the RVM and SVM for RSIR using deep features. The robust deep features extracted using the RAE with dimensionality reduction and preserving the affinity between the data and relationship help in achieving better classification results. The RAE-HHSKC framework provides competing results by bringing together the better qualities of both the SKLM in classifying highly overlapping classes. Hence, the likelihood of using a hybrid approach is effective for the high-dimensional RS data.

5. CONCLUSION

A new retrieval strategy using the RAE-HHSKC framework is formulated for the high dimensional RSI. The recommended retrieval strategy extends the capabilities of the RVM and SVM in a hybrid fashion to resolve the multiclass problem. The robust deep features extracted using the RAE improves the overall efficiency of the retrieval model. The probabilistic behavior of the RVM based classification outcome may be of considerable value. The RAE-HHSKC model achieved state-of-the-art results concerning the precision, recall, and F1-score for the two RS datasets. The UCMD dataset achieved a precision of 95.15%, and the RS-19 dataset achieved a precision of 94.59%, respectively. The results attained show that using the RAE-HHSKC framework is promising for the high-dimensional RS datasets. Although the performances of the RAE-HHSKC method are satisfactory, the method can be extended to a large-scale multi-label scenario as our future work.

AUTHORS' CONTRIBUTIONS

Conceptualization, methodology, and writing of the work done by Sudha S K and the analysis and verification done by Aji S. All authors have read and agreed to the published version of the manuscript.

ACKNOWLEDGMENTS

We would like to thank the University of Kerala for providing the facilities for doing this research under the University JRF scheme.

REFERENCES

[1] Rajan, S.; Ghosh, J.; and Crawford, M., An Active-Learning Approach to Hyperspectral Data Classification, IEEE Transactions on Geoscience and Remote Sensing, (2008), 46, pp. 1231–1242, DOI: 10.1109/TGRS.2007.910220.

[2] Osman Emre Dai, Begum Demir, Bulent Sankur, and Lorenzo Bruzzone, A Novel System for Content based Retrieval of Single and Multi Label High Dimensional Remote Sensing Images, IEEE Journal of Selected Topics in Applied Earth Observations and Remote Sensing, (2018), 11(7), pp. 2473-2490, DOI: 10.1109/JSTARS.2018.2832985.

[3] C. Ma, F. Chen, J. Yang, J. Liu, W. Xia, and X. Li, A Remote Sensing Image Retrieval Model based on An Ensemble-Neural-Networks, Big Earth Data, (2018), 2(4), pp. 351-367, DOI:10.1080/20964471.2019.1570815.

[4] AC Grivei, A. Radoi, C. Vaduva, and M. Datcu, An Active-Learning Approach to the Query-by-Example Retrieval in Remote Sensing Images, International Conference on Communications (COMM), (2016), pp. 377-380, DOI:10.1109/ICComm.2016.7528339.

[5] Min-Sub Yun, Woo-Jeoung Nam, and Seong-Whan Lee, Coarse-to-Fine Deep Metric Learning for Remote Sensing Image Retrieval, MDPI, Remote Sensing, (2020), 12(219), pp. 1-20, DOI:10.3390/rs12020219.

[6] Yishu Liu, Liwang Ding, Conghui Chen, and Yingbin Liu, Similarity-based Unsupervised Deep Transfer Learning for Remote Sensing Image Retrieval, IEEE Transactions on Geoscience and Remote Sensing, (2020), pp. 1 –18, DOI:10.1109/TGRS.2020.2984703.

[7] Pingping Liu, Guixia Gou, Xue Shan, Dan Tao, and Qiuzhan Zhou, Global Optimal Structured Embedding Learning for Remote Sensing Image Retrieval, MDPI, Sensors, (2020), 20, 291, DOI:10.3390/s20010291.

[8] Zheng Zhuo and Zhong Zhou, Remote Sensing Image Retrieval with Gabor-CA-ResNet and Split-Based Deep Feature Transform Network, MDPI, Remote Sensing, (2021), 13, 869, DOI:10.3390/rs13050869.

[9] Rui Cao, Qian Zhang, Jiasong Zhu, Qing Li, Qingquan Li, Bozhi Liu, and Guoping Qiu, Enhancing Remote Sensing Image Retrieval with Triplet Deep Metric Learning Network, International Journal of Remote Sensing, (2019), 41(2), pp. 740-751, DOI:10.1080/2150704X.2019.1647368.

[10] Weixun Zhou, Zhenfeng Shao, Chunyuan Diao, and Qimin Cheng, High-Resolution Remote-Sensing Imagery Retrieval using Sparse Features by Auto-Encoder, Remote Sensing Letters, (2015), 6(10), pp. 775–783, DOI:10.1080/2150704X.2015.1074756.

[11] Ferecatu, M.; and Boujemaa, N., Interactive Remote Sensing Image Retrieval Using Active Relevance Feedback, IEEE Transactions on Geoscience and Remote Sensing, (2007), 45(4), pp. 818–826, DOI:10.1109/TGRS.2007.892007.

[12] Duan, J.; Ma, C.; Liu, S. B.; and Zhang, J., The Remote Sensing Image Retrieval Based on Multi-Feature, In: Proc. of SPIE Image and Signal Processing for Remote Sensing, (2013), 8892, 88921X 6, DOI:10.1117/12.202147.

[13] Ma C.; Dai Q.; Liu J.; Liu S.; and Yang J., An Improved SVM Model for Relevance- Feedback in Remote Sensing Image Retrieval, International Journal of Digital Earth, (2014), 7(9), pp. 725–745, DOI:10.1080/17538947.2013.781238.

[14] Demir, B.; and Bruzzone, L., A Novel Active-Learning Method in Relevance Feedback for Content based Remote Sensing Image Retrieval, IEEE Transactions on Geoscience and Remote Sensing, (2014), 53(5), pp. 2323–2334.

[15] Wang, Y.; Zhang, L.; Tong, X.; Zhang, L.; Zhang, Z.; and Liu, H., A Three Layered Graph- based Learning Approach for Remote Sensing Image Retrieval, IEEE Transactions on Geoscience and Remote Sensing, (2016), 54(10), pp. 6020–6034.

[16] Yansheng Li, Yongjun Zhang, Chao Tao, and Hu Zhu, Content based High Resolution Remote Sensing Image Retrieval via Un-supervised Feature Learning and Collaborative Affinity Metric Fusion, MDPI, Remote Sensing (2016), 8(9), 709.

[17] Tang, X.; Jiao, L.; Emery, W. J.; Liu, F.; and Zhang, D., Two-stage Re-Ranking for Remote Sensing Image Retrieval, IEEE Transactions on Geoscience and Remote Sensing (2017), 55(10), pp. 5798–5817, DOI: 10.1109/TGRS.2017.2714676.

[18] Napoletano, P., Visual Descriptors for Content based Retrieval of Remote Sensing Images, International Journal of Remote Sensing (2017), 39(5), pp. 1–34.

[19] Demir, B., and Bruzzone, L., Hashing-based Scalable Remote Sensing Image Search and Retrieval in Large-Archives, IEEE Transactions on Geoscience and Remote Sensing, (2015), 54(2), pp. 892–904.

[20] Tang, X.; and Jiao, L., Fusion Similarity-based Reranking for SAR Image Retrieval, IEEE Geoscience and Remote Sensing Letters, (2017), 14(2), pp. 242–246, DOI: 10.1109/LGRS.2016.2636819.

[21] Peng Li, Lirong Han, Xuanwen Tao, and Xiaoyu Zhang, Hashing Nets for Hashing: A Quantized Deep Learning to Hash Framework for Remote Sensing Image Retrieval, IEEE Transactions on Geoscience and Remote Sensing, (2020), 58(10), pp. 7331-7345, DOI: 10.1109/TGRS.2020.2981997.

[22] Z. Shao, W. Zhou, X. Deng, M. Zhang, and Q. Cheng, Multilabel Remote Sensing Image Retrieval Based on Fully Convolutional Network, in IEEE Journal of Selected Topics in Applied Earth Observations and Remote Sensing, 13, pp. 318-328, (2020), DOI: 10.1109/JSTARS.2019.2961634.

[23] Sudheer Devulapalli and Rajakumar Krishnan, Remote Sensing Image Retrieval by Integrating Automated Deep feature Extraction and Handicrafted Features using Curvelet Transform, Journal of Applied Remote Sensing, 15(1), 016504, (2021), DOI:10.1117/1.JRS.15.016504.

[24] L. Fan, H. Zhao, and H. Zhao, Global Optimization: Combining Local Loss With Result Ranking Loss in Remote Sensing Image Retrieval, in IEEE Transactions on Geoscience and Remote Sensing, (2020), DOI: 10.1109/TGRS.2020.3029334.

[25] F. Ye, W. Luo, M. Dong, D. Li and W. Min, Content based Remote Sensing Image Retrieval Based on Fuzzy-Rules and a Fuzzy-Distance, in IEEE Geoscience and Remote Sensing Letters, (2020), DOI: 10.1109/LGRS.2020.3030858.

[26] Y. Liu, C. Chen, Z. Han, L. Ding, and Y. Liu, High-Resolution Remote Sensing Image Retrieval Based on Classification-Similarity Networks and Double Fusion, in IEEE Journal of Selected Topics in Applied Earth Observations and Remote Sensing, (2020),13, pp. 1119-1133, DOI: 10.1109/JSTARS.2020.2981372.

[27] U. Chaudhuri, B. Banerjee, A. Bhattacharya, and M. Datcu, A Zero-Shot Sketch-Based Intermodal Object Retrieval Scheme for Remote Sensing Images, in IEEE Geoscience and Remote Sensing Letters, DOI: 10.1109/LGRS.2021.3056392.

[28] H. Zhao, L. Yuan, H. Zhao, and Z. Wang, Global-Aware Ranking Deep Metric Learning for Remote Sensing Image Retrieval, in IEEE Geoscience and Remote Sensing Letters, (2021), DOI: 10.1109/LGRS.2021.3059908.

[29] G.E. Hinton, S. Osindero, and Y.W. The, A Fast-Learning Algorithm for Deep Belief Nets, Neural Computation. (2006), 18(7), 1527–1554, DOI: 10.1162/neco.2006.18.7.1527.

[30] Chen, Y.; Lin, Z.; Zhao, X.; Wang, G.; and Gu, Y., Deep Learning-based Classification of Hyperspectral Data, IEEE Journal of Selected Topics in Applied Earth Observations and Remote Sensing, (2014), 7, pp. 2094–2107, DOI: 10.1109/JSTARS.2014.2329330.

[31] Meng, Q., Catchpoole, D., Skillicom, D., and Kennedy, P. J., Relational Autoencoder for Feature Extraction, International Joint Conference on Neural Networks (IJCNN), (2017), pp. 364-371, DOI: 10.1109/IJCNN.2017.7965877.

[32] Ce Zhang, Xin Pan, Huapeng Li, Andy Gardiner, Isabel Sargent, Jonathon Hare, and Peter M. Atkinson, A Hybrid MLP-CNN Classifier for Very Fine Resolution Remotely Sensed Image Classification, ISPRS Journal of Photogrammetry and Remote Sensing, (2017), DOI:10.1016/j.isprsjprs.2017.07.014.

[33] Shoulin Yin, Ye Zhang, and Shahid Karim, Region Search Based On Hybrid Convolutional Neural Network in Optical Remote Sensing Images, International Journal of Distributed Sensor Networks, (2019), 15(5), DOI:10.1177/1550147719852036.

[34] V. Vapnik, The Nature of Statistical Learning Theory, Springer, (1999).

[35] M. Tipping, Sparse Bayesian Learning and The Relevance Vector Machine, Journal of Machine Learning Research, (2001), 1, pp. 211–244.

[36] Foody G. M., RVM-based Multiclass Classification of Remotely Sensed Data, International Journal of Remote Sensing, (2008), 29, pp. 1817-1823, DOI:10.1080/01431160701822115.

[37] W. Huilan, L. Guodong, and P. Zhaobang, Multiclass Image Recognition Based on Relevance Vector Machine, In: Intelligent Systems and Applications, (2009), pp. 1 – 4, DOI: 10.1109/IWISA.2009.5072963.

[38] Yang, Y.; and Newsam, S., Bag-of-Visual-Words and Spatial Extensions for Land use Classification, In: Proceedings of the 18th SIGSPATIAL - International Conference on Advances in Geographic Information Systems - San Jose, CA, USA, (2010), pp. 270–279, DOI:10.1145/1869790.1869829.

[39] Dai, Dengxin, and Wen Yang, Satellite Image Classification via Two-Layer Sparse Coding with Biased Image Representation, Geoscience, and Remote Sensing Letters. (2011), 8 (1), pp. 173–176, DOI:10.1109/LGRS.2010.2055033.

[40] Bindita Chaudhuri, Begum Demir, Lorenzo Bruzzone, and Subhasis Chaudhuri, Region based Retrieval of Remote Sensing Images using an Unsupervised Graph Theoretic Approach, IEEE Geoscience, and Remote Sensing Letters. (2016), 13(7), pp. 987-991, DOI: 10.1109/LGRS.2016.2558289.

[41] Yuebin Wang, Liqiang Zhang, Xiaohua Tong, Liang Zhang, Zhenxin Zhang, Hao Liu, Xiaoyue Xing, and P. Takis Mathiopoulos, A Three-Layered Graph-Based Learning Approach for Remote Sensing Image Retrieval, IEEE Transactions on Geoscience and Remote Sensing, (2016), 54(10), pp. 6020-6034, DOI: 10.1109/TGRS.2016.2579648.

[42] Ushasi Chaudhuri, Biplab Banerjee, and Avik Bhattacharya, Siamese Graph-Convolutional Network for Content-based Remote Sensing Image Retrieval, Computer Vision and Image Understanding. (2019), 184, pp. 22–30, DOI:10.1016/j.cviu.2019.04.004.

[43] Weixun Zhou, Xueqing Deng, and Zhenfeng Shao, Region Convolutional Features for Multi-Label Remote Sensing Image Retrieval, Computer Vision and Pattern Recognition, (2020), 13, pp. 318-328, DOI:10.1109/JSTARS.2019.2961634.

[44] Weixun Zhou, Shawn Newsam, Congmin Li, and Zhenfeng Shao, Learning Low-Dimensional Convolutional Neural Networks for High-Resolution Remote Sensing Image Retrieval,

MDPI, Remote Sensing, (2017), 9(5), 489, DOI:10.3390/rs9050489.

[45] Xin-Yi Tong, Gui-Song Xia, Fan Hu, Yanfei Zhong, Mihai Datcu, and Liangpei Zhang, Exploiting Deep Features for Remote Sensing Image Retrieval- A Systematic Investigation, (2019), IEEE Transactions on Big Data, 6(3), 507-521, DOI: 10.1109/tbdata.2019.2948924.

[46] Rajendrakumar, Shiny, and V. K. Parvati. "Automation of irrigation system through embedded computing technology." In *Proceedings of the 3rd International Conference on Cryptography, Security and Privacy*, pp. 289-293. 2019.

[47] Kumar, M. Keerthi, B. D. Parameshachari, S. Prabu, and Silvia liberata Ullo. "Comparative Analysis to Identify Efficient Technique for Interfacing BCI System." In *IOP Conference Series: Materials Science and Engineering*, vol. 925, no. 1, p. 012062. IOP Publishing, 2020.

[48] K. Yu, L. Tan, X. Shang, J. Huang, G. Srivastava and P. Chatterjee, "Efficient and Privacy-Preserving Medical Research Support Platform Against COVID-19: A Blockchain-Based Approach", IEEE Consumer Electronics Magazine, doi: 10.1109/MCE.2020.3035520.

[49] Z. Guo, Y. Shen, A. K. Bashir, M. Imran, N. Kumar, D. Zhang and K. Yu, "Robust Spammer Detection Using Collaborative Neural Network in Internet of Thing Applications", IEEE Internet of Things Journal, vol. 8, no. 12, pp. 9549-9558, 15 June15, 2021, doi: 10.1109/JIOT.2020.3003802.

[50] Naeem, Muhammad Ali, Tu N. Nguyen, Rashid Ali, Korhan Cengiz, Yahui Meng, and Tahir Khurshaid. "Hybrid Cache Management in IoT-based Named Data Networking." *IEEE Internet of Things Journal* (2021).

[51] Le, Ngoc Tuyen, Jing-Wein Wang, Duc Huy Le, Chih-Chiang Wang, and Tu N. Nguyen. "Fingerprint enhancement based on tensor of wavelet subbands for classification." *IEEE Access* 8 (2020): 6602-6615.

[52] Arun, M., E. Baraneetharan, A. Kanchana, and S. Prabu. "Detection and monitoring of the asymptotic COVID-19 patients using IoT devices and sensors." *International Journal of Pervasive Computing and Communications* (2020).

[53] Kumar, M. Keerthi, B. D. Parameshachari, S. Prabu, and Silvia liberata Ullo. "Comparative Analysis to Identify Efficient Technique for Interfacing BCI System." In *IOP Conference Series: Materials Science and Engineering*, vol. 925, no. 1, p. 012062. IOP Publishing, 2020.

[54] L. Tan, N. Shi, K. Yu, M. Aloqaily, Y. Jararweh, "A Blockchain-Empowered Access Control Framework for Smart Devices in Green Internet of Things", ACM Transactions on Internet Technology, vol. 21, no. 3, pp. 1-20, 2021,https://doi.org/10.1145/3433542.

[55] Z. Guo, A. K. Bashir, K. Yu, J. C. Lin, Y. Shen, "Graph Embedding-based Intelligent Industrial Decision for Complex Sewage Treatment Processes", International Journal of Intelligent Systems，2021, doi: 10.1002/int.22540.

[56] Do, Dinh-Thuan, Tu Anh Le, Tu N. Nguyen, Xingwang Li, and Khaled M. Rabie. "Joint impacts of imperfect CSI and imperfect SIC in cognitive radio-assisted NOMA-V2X communications." *IEEE Access* 8 (2020): 128629-128645.

[57] Subramani, Prabu, K. Srinivas, R. Sujatha, and B. D. Parameshachari. "Prediction of muscular paralysis disease based on hybrid feature extraction with machine learning technique for COVID-19 and post-COVID-19 patients." *Personal and Ubiquitous Computing* (2021): 1-14.

[58] N. Shi, L. Tan, W. Li, X. Qi, K. Yu, "A Blockchain-Empowered AAA Scheme in the Large-Scale HetNet", Digital Communications and Networks, https://doi.org/10.1016/j.dcan.2020.10.002.

[59] Y. Sun, J. Liu, K. Yu, M. Alazab, K. Lin, "PMRSS: Privacy-preserving Medical Record Searching Scheme for Intelligent Diagnosis in IoT Healthcare", IEEE Transactions on Industrial Informatics, doi: 10.1109/TII.2021.3070544.